THE ASTROPHYSICAL JOURNAL, 390:345–349, 1992 May 10

A2163: AN EXCEPTIONALLY HOT CLUSTER OF GALAXIES

M. ARNAUD,[1] J. P. HUGHES, W. FORMAN, AND C. JONES
Harvard-Smithsonian Center for Astrophysics, 60 Garden Street, Cambridge, MA 02138
M. LACHIEZE-REY
Service d'Astrophysique, CEN Saclay, 91191 Gif sur Yvette Cedex, France
K. YAMASHITA
Institute of Space and Astronautical Science, Sagamihara, Kanagawa 229, Japan
AND
I. HATSUKADE
Faculty of Engineering, Miyazaki University, Miyazaki 889-20, Japan
Received 1991 May 10; accepted 1991 October 8

ABSTRACT

We measured the X-ray spectrum of the distant galaxy cluster A2163 in the energy range 1–18 keV with the *Ginga* satellite. A combined analysis of these data with data previously obtained with the *Einstein Observatory* is presented. The mean temperature and X-ray luminosity we derive are exceptionally high compared to other clusters: $kT = 12.9$ keV, L_X (2–10 keV) = 3.5×10^{45} ergs s^{-1} for $z = 0.15$, as are the gas mass (6.7×10^{14} $M_\odot$) and binding mass (25×10^{14} $M_\odot$). The very existence of such a cluster can provide interesting constraints on the relative distribution of "visible" mass and dark matter, an important parameter in cold dark matter models for formation of structure in the universe.

Subject headings: dark matter — galaxies: clustering — X-rays: galaxies

1. INTRODUCTION

The sensitivity of the proportional counters (Turner et al. 1989) on board the Japanese satellite *Ginga* permits, for the first time, the precise measurement of the temperature and heavy element abundance in the intergalactic medium of clusters with redshift $z > 0.1$ (Hatsukade 1989; McHardy et al. 1989; Arnaud et al. 1991; Hughes & Tanaka 1991). These parameters are essential for our understanding of the formation and evolution of galaxy clusters (Perrenod 1980; Cavaliere et al. 1986; Schaeffer & Silk 1988; Lilje 1990; Arnaud et al. 1991). We report here spectroscopic observations of the distant cluster A2163 with the *Ginga* satellite. These new data, combined with data (image and spectra) previously obtained with the *Einstein* satellite, are used to constrain the temperature, iron abundance, luminosity, gas mass, and binding mass of A2163 (§§ 2 and 3). The implications of our results for cosmological models of the formation of structure in the universe are discussed in § 4.

2. OBSERVATIONS AND DATA REDUCTION

A2163 was observed with the *Ginga* LAC (large area counters) on 1989 August 21. The LAC experiment (Turner et al. 1989) consists of eight identical collimated proportional counters, with a total geometrical area of 4000 cm^2 and a $1° \times 2°$ field of view. Each counter has two layers, the TOP layer sensitive to X-rays in the energy range 1–20 keV and the MID layer sensitive to X-rays above 5 keV. Several slew scans around the position of the cluster were performed. The source was clearly detected at the expected position of the cluster, and the scan profile obtained is consistent with an unresolved source viewed by the LAC collimator of intensity 13.5 ± 1.2 counts s^{-1} (TOP layer, 1–17 keV). No other source was detected in these scanning data in the vicinity of the cluster. After discarding the data corresponding to high background levels (Arnaud et al. 1991; Hughes & Tanaka 1991) we were left with $\sim$12,000 s of useful observation time in pointing mode. We subtracted the background in TOP and MID layer data using standard techniques (Arnaud et al. 1991; Hayashida et al. 1989) as we describe below. The energy scale was calibrated by fitting the Ag Kα line apparent in the raw spectra at 22.1 keV, arising from fluorescence in the *Ginga* collimator. The 1 σ error on the detector gain, as estimated from the 1 σ error on the fitted line energy, is less than 1%. Finally, we took the position of the cluster determined from X-ray imaging data (see below) as the reference for the aspect correction. A significant flux was observed in both the TOP (1–17 keV) and MID (6–18 keV) layers of the LAC, and the corresponding spectra are used in our further analysis (see Fig. 1). The count rate in the TOP layer, 14.4 counts s^{-1}, is consistent with the value deduced from the scan data.

A2163 was previously observed by the IPC (Ulmer, Kowalski, & Cruddace 1986) and the MPC on board the *Einstein* satellite, for 1517.3 s on 1979 August 17. An extended X-ray source apparent in the IPC image is centered at $16^h13^m6^s$, $-6°1'20''$ (1950). Background was subtracted from the IPC data using a gain-matched empty field (deep survey field I27). The cluster surface brightness profile obtained (see Fig. 2) is well fitted by the expression

$$\Sigma = \Sigma_0 \left[1 + \left(\frac{r}{R_c}\right)^2\right]^{-3\beta + 1/2} , \quad (1)$$

where r is the distance to the cluster center and R_c is the core radius. We derived $R_c = 1.15$ (-0.32, $+0.39$) arcmin and $\beta = 0.59$ (-0.06, $+0.08$) (90% confidence level). To extract the

[1] Also at Service d'Astrophysique, CEN Saclay.

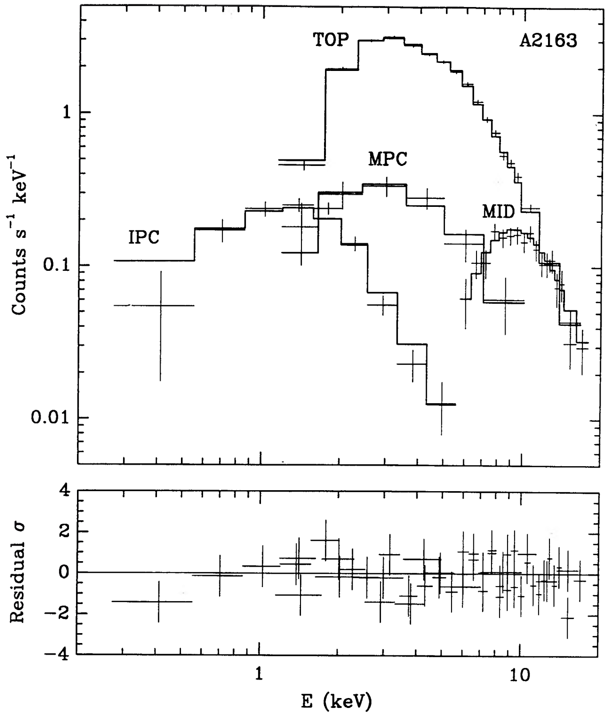

FIG. 1.—The top figure corresonds to the A2163 spectra as measured with the *Einstein* satellite (IPC and MPC instruments) and with the *Ginga* satellite (TOP and MID layers of the proportional counter array). *Crosses*: data points with error bars. Spectrum at the top of the figure: TOP layer spectrum. Spectra at the bottom of the figures, from left to right: IPC, MPC and MID layer spectrum. *Full lines*: the best-fit isothermal model for $z = 0.25$: $N_H = 2.7 \times 10^{21}$ cm^{-2}, $kT = 14.7$ keV, iron abundance = 0.35, $L_x = 9.8 \times 10^{45}$ ergs s^{-1}. The bottom figure indicates the deviation between data and model.

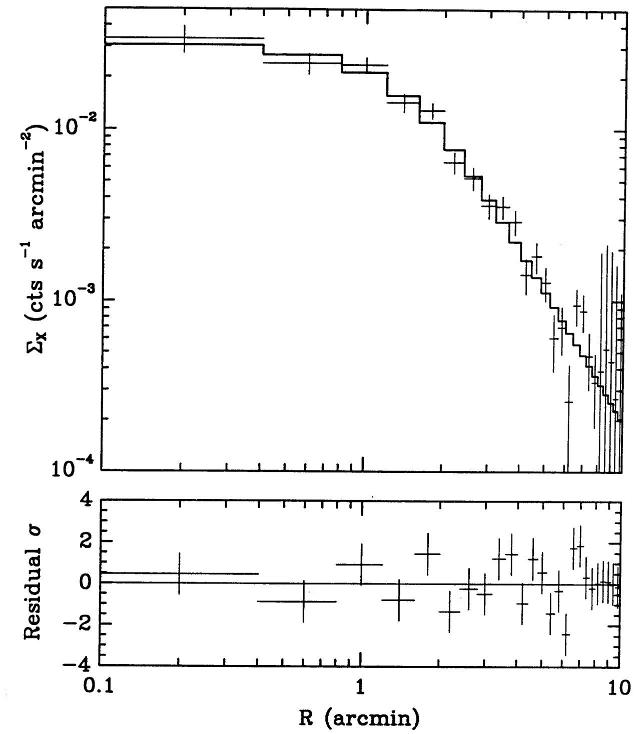

FIG. 2.—The top figure displays the azimuthally averaged surface brightness vs. the distance to the cluster center. *Crosses*: data points with error bars from IPC; *full line*: best-fit β model (core radius = 1'.15 and $\beta = 0.59$) convolved with the IPC point response. The best-fit χ^2 is 27.6 for 21 degrees of freedom. The bottom figure indicates the deviation between data and model.

IPC spectrum, we considered only emission from within a 7'.5 radius from the cluster center to optimize the signal-to-noise ratio. We added an additional uncertainty equivalent to 20% of the background rate in quadrature to the statistical error, to account for possible variation of IPC background from field to field (Hughes & Tanaka 1991). The IPC count rate thus derived is 0.487 ± 0.025 counts s^{-1} (in the energy range 0.27–4.3 keV). The MPC also clearly detected the source with a count rate of 1.57 ± 0.19 counts s^{-1} (1–10 keV). Both MPC and IPC spectra are shown in Figure 1.

From optical measurements, A2163 is a rich cluster ($N_{\rm Abell} = 119$ galaxies) of Rood and Sastry class I (Struble & Rood 1987). It is a distant cluster ($z \sim 0.2$) though the exact value of the redshift is still uncertain. The redshift (0.1698) given by Kowalski, Ulmer, & Cruddace (1983) is based on the measurement of one galaxy only, A2163 G1, which lies outside the X-ray emitting region corresponding to the cluster: it is located at $16^h12^m46^s$, $-6°9'50''$ (1950), 9' from the cluster center. Another galaxy, A2163 G5, considered by Kowalski et al. to be a background galaxy, has a redshift of 0.2163 and is nearer the cluster center, 4' away. The X-ray data can constrain the redshift since the iron line is clearly detected in the TOP layer spectrum (see below). However, the uncertainties are large: a redshift in the range 0.14–0.26 is allowed at the 90% confidence level, if one fits the TOP layer spectrum with a redshifted isothermal plasma emission model (Raymond & Smith 1977; Raymond 1985). In view of these uncertainties[2] we choose to present results obtained by assuming two extreme values of the redshift: $z = 0.15$ and $z = 0.25$.

[2] A more accurate determination of the redshift is scheduled at the CFHT.

3. MODEL FITTING

We fit all the available spectra (IPC, MPC, and *Ginga*, see Fig. 1) with the redshifted isothermal plasma emission model of Raymond & Smith (1977). The free parameters are the hydrogen column density in the line of sight N_H, the overall normalization, the temperature kT, and the iron abundance in the intracluster medium (ICM), the abundances of all heavy elements with $Z > 2$ (C, N, O, ...) being varied in unison. We introduced a relative normalization between the IPC and *Ginga* spectra, and between the MPC and *Ginga* spectra to check the consistency between *Einstein* and *Ginga* observations. An excellent agreement between the isothermal model and the data is obtained (reduced $\chi^2 = 0.8$ for $\nu = 44$ degrees of freedom). The best-fit parameters together with the 90% confidence errors are given in Table 1, and the best-fit spectra are plotted in Figure 1. As discussed in a previous paper (Arnaud et al. 1991), the uncertainties due to the choice of the underlying atomic physics are negligible. We checked this point by comparing the results obtained by using the Mewe, Gronenshild, & van den Oord (1985) and Mewe, Lemen, & van den Oord (1986) model and the Masai (1984a, b) model instead of the Raymond & Smith model (1977): the discrepancies in the best-fit temperature, and iron abundance (relative to solar) are typically 0.5 keV and 0.05 respectively and are much smaller than the 90% confidence level errors on these parameters.

The agreement between the *Ginga* data and the *Einstein* data is excellent. The normalization between the MPC and *Ginga* data is consistent with 1, if we take into account the large error

TABLE 1

DERIVED PHYSICAL PARAMETERS FROM PLASMA MODEL FIT FOR A2163

Parameter[a]	$z = 0.15$	$z = 0.25$
Spectral Data		
L_X(2–10 keV) (ergs s^{-1})[b]	3.5×10^{45}	10×10^{45}
kT (keV)	12.9(−0.8, +1.1)	14.7(−1.1, +1.0)
Iron abundance[c]	0.33(−0.13, +0.13)	0.35(−0.14, +0.15)
log (N_H, cm^{-2})	21.44(−0.15, +0.13)	21.42(−0.16, +0.14)
Relative normalization: IPC/*Ginga*	0.92	0.91
Relative normalization: MPC/*Ginga*	0.84	0.84
Best-fit χ^2 (44 dof)	33.3	35.2
Imaging Data		
L_X(0.5–4.5 keV) (ergs s^{-1})[b]	2.7×10^{45}	7.9×10^{45}
β	0.59(−0.06, +0.08)	0.59(−0.06, +0.08)
Core radius (arcmin)[b]	1.15(−0.32, +0.39)arcmin 0.24 Mpc	1.15 (−0.32, +0.39) arcmin 0.34 Mpc
Central electronic density (10^{-3} cm^{-3})[b,d]	7.0	6.8
Cooling time (10^{10} yr)[b,d]	0.95	1.0
Gas mass inside 3 Mpc radius (10^{14} $M_\odot$)[b,d]	6.7	12.0
Binding mass (10^{14} $M_\odot$)[b,d]	25.0	28.0

[a] Errors at 90% confidence level.
[b] Assuming $H_0 = 50$ km s^{-1} Mpc^{-1} and $q_0 = 0.5$.
[c] Relative to cosmic: [Fe/H] $= 4 \times 10^{-5}$.
[d] Adopting the best-fit temperature and hydrogen column density.

bars on the MPC data. The 8% discrepancies in normalization between the IPC and *Ginga* can be accounted for by the uncertainty ($\sim 5\%$) in the overall flux calibration of each instrument (Hughes & Tanaka 1991) and by the choice of the integration region for the IPC spectrum. Indeed, the IPC spectrum corresponds to the flux inside about 7 core radii, whereas the *Ginga* spectrum corresponds to the total emission. If we adopt the density profile deduced from imaging data and assume that the cluster has an actual extent of 10 core radii, we expect 10% less flux in the IPC spectrum as compared to that from *Ginga*. We *also* note that the best-fit values for the parameters (kT, [Fe/H]), *obtained* by fitting the *Ginga* data alone on one hand and the *Ginga* data together with the *Einstein* data on the other, are the same: there is less than 0.05 keV discrepancy for kT, and 0.005 for [Fe/H].

The best-fit value of N_H deduced from the X-ray data exceeds the value for the atomic hydrogen column density, 1.1×10^{21} cm^{-2}, obtained from 21 cm measurements (Stark et al. 1983) by about a factor of 2. Since the spectral shape is sensitive to the total quantity of absorbing material in the line of sight, we have also considered the presence of Galactic molecular hydrogen in the direction of the cluster. We can estimate the molecular hydrogen column density N_{H_2} using as a tracer the CO molecule (Dame et al. 1987). Measurements of the CO emission line at 2.6 mm were kindly performed by T. Dame (private communication) using the 1.2 m CfA radio telescope. He derived a firm upper limit of $N_{H_2} < 1.0 \times 10^{20}$ cm^{-2}, clearly demonstrating that the atomic hydrogen is by far the dominant absorbing material in the direction of A2163. The 21 cm survey may have underestimated the hydrogen column density in the direction of A2163 because of its low spatial resolution (A. Stark, private communication): there is considerable structure in the interstellar medium (ISM) at the scale of the resolution of the survey (1°.5) and a factor of 2 enhancement of the column density in a particular direction over the surrounding 1°.5 region is possible. Increased absorption above that predicted from 21 cm measurements has been reported by White et al. (1991) for a large sample of clusters. The origin of this excess absorption is uncertain and could either be galactic or associated with the clusters themselves. We will simply note here that a barely acceptable spectral fit for A2163 (reduced $\chi^2 = 1.0$ for $\nu = 45$) is also obtained if one arbitrarily fixes the N_H value to that deduced from 21 cm measurements; however, in that case the temperature obtained is higher (by ~ 1 keV) as is the heavy element abundance (by ~ 0.1) because a harder spectrum can mimic lower absorption.

4. DISCUSSION

The derived best-fit (emission-weighted average) temperature and X-ray luminosity are exceptionally high: $kT = 12.9$ keV, $L_X(2\text{–}10 \text{ keV}) = 3.5 \times 10^{45}$ ergs s^{-1} for $z = 0.15$, and $kT = 14.7$ keV, $L_X(2\text{–}10 \text{ keV}) = 10 \times 10^{45}$ ergs s^{-1} for $z = 0.25$. The temperature is greater for the higher redshift, since the energies, and therefore the temperature obtained, roughly scale as $(1 + z)$. As a consequence, the derived iron abundance also increases with the redshift, the theoretical equivalent width of the iron line being a decreasing function of the temperature (e.g., Arnaud et al. 1991). However, this effect is small: [Fe/H] $= 0.33$ for $z = 0.15$ and [Fe/H] $= 0.35$ for $z = 0.25$. The luminosity is of course very sensitive to the redshift, due to the distance effect. In any case, even if one assumes a very conservative value for the redshift ($z = 0.15$), A2163 remains quite exceptional. Let us recall that the hottest and most luminous known clusters (like Ophiucus [Arnaud et al. 1987; Johnson et al. 1981]) have mean (emission-weighted) temperatures and luminosities not exceeding 9 keV and 2×10^{45} ergs s^{-1}, respectively, whereas a temperature of 7 keV is more typical of rich clusters (e.g., Edge 1989).

From the imaging data and the temperature deduced from the spectral data, we derived the gas mass and the binding mass (inside a radius of 3 Mpc) assuming isothermality. These masses as well as the cluster central gas density and cooling time are given in Table 1 for the best-fit parameters. Again

A2163 appears to be quite atypical: even for $z = 0.15$ the gas mass and binding mass are respectively 2.5 and 1.8 times the corresponding masses ($2.7 \times 10^{14}\ M_\odot$ and $1.4 \times 10^{15}\ M_\odot$, Hughes, Gorenstein, & Fabricant 1988; Hughes 1989) of a very rich cluster such as Coma.

Before discussing the physical implication of these results, we will now further examine their accuracy. The temperature is essentially constrained by the *Ginga* data. Such high temperatures could be artificially obtained from an incorrect background subtraction in the *Ginga* data (leaving extra counts at high energy) or if a hard source active galactic nucleus (AGN) were present in the field of view, contaminating the observation. We can rule out these possibilities for several reasons.

1. Two independent techniques can be used for background subtraction: (1) subtraction using a blank field observation (Arnaud et al. 1991; Hayashida et al. 1989) which was adopted above and (2) subtraction of the background model developed by Hayashida et al. (1989). The spectra obtained from the two methods are consistent and there are no significant differences in the derived best-fit values: the change is less than 0.14 keV for the temperature, 0.08 for the relative iron abudance, and 4% for the luminosity.

2. Since the background is not the same for the LAC TOP and MID layer, an incorrect background subtraction would a priori yield inconsistent MID and TOP spectra. This is not the case. An excellent fit is obtained by fitting at the same time the TOP and MID spectra with the isothermal model: the reduced χ^2 is 0.8 (for $\nu = 31$).

3. A pure power-law spectrum, typical of AGN emission, can be rejected at the 99.99% confidence level: a χ^2 of 94 for 32 degrees of freedom is obtained if one tries to fit the *Ginga* spectra (TOP and MID simultaneously) by such a model. This is due to the clear contribution of the iron line in the TOP layer spectrum. Moreover, there is extended X-ray emission seen on the IPC image. These points, added to the consistencies between the *Einstein* and *Ginga* spectral data and between *Ginga* scanning and pointing data, indicate that the predominant X-ray emission seen by *Ginga* comes from the hot intracluster gas. To investigate further the possible contribution of AGN–type emission in the spectrum, we tried to fit the spectral data by a composite model: thermal emission with the added contribution of power law with the canonical slope of 1.7 (Turner & Pounds 1989). We considered two cases: (1) an AGN at the center of the IPC image, corresponding in all likelihood to a cluster with an active central galaxy and (2) an AGN not contributing to the emission seen by the IPC, i.e., not linked to the cluster, but present in the large field of view of the LAC experiment. In both cases the best fit for the normalization of the power-law component is virtually zero (its contribution is less than 1%), and of course the parameters obtained for the thermal component are the same as those obtained without the power-law component. Note that we obtained the same result for the best fit, with the power-law exponent varying as a free parameter. For case (1) the temperature cannot be lowered by more than 0.48 keV (at the 90% confidence level) as compared with the temperature obtained without the power-law component if we also take into account the strong constraint given by the IPC imaging data: the contribution of a point source at the center of the cluster cannot exceed 10% of the total emission seen by IPC. For case (2) the contribution of the power-law component cannot exceed 12% (in the 2–10 keV energy range and at the 90% confidence level) and the maximum allowed decrease of the temperature is 0.56 keV. Finally some peculiar AGNs present a heavily absorbed power-law spectrum (Turner & Pounds 1989) and their emission could contribute in the *Ginga* range without contributing significantly in the IPC range. We thus also tried to add to the thermal component a power-law component with a significant intrinsic absorbing column density $N_{\rm H} = 10^{23}$ cm^{-2} (the maximum value observed in AGNs (Turner & Pounds 1989; Warwick et al. 1989)). Again zero is obtained for the normalization of the power-law component.

4. Finally we note that the atypical properties of A2163 are readily apparent in the data, even without detailed analysis: the observed TOP layer count rate for A2163 is 3.2 times higher than the corresponding count rates we previously observed for A2507 (Arnaud et al. 1991) which has a similar redshift ($z = 0.196$) and a luminosity of 1.7×10^{45} ergs s^{-1} and the very detection of a significant flux from A2163 in the *Ginga* MID layer, sensitive to high-energy photons, already indicates an exceptionally hard spectrum. Moreover, the fact that both the temperature and luminosity are high is consistent with the correlation observed between these two quantities in clusters: the relationship established between these two quantities by Edge (1989; see also Mushotzky et al. 1978) predicts a luminosity of 4×10^{45} ergs s^{-1} for $kT = 12.9$ keV and $L_X \sim 6 \times 10^{45}$ ergs s^{-1} for $kT = 14.7$ keV.

The existence of massive systems like A2163 has implications for cosmological models of the formation of structure in the universe. In particular, in the context of cold dark matter (CDM) models of the universe with biased galaxy formation, the total cluster mass and intracluster gas temperature (after virialization) are related by

$$kT = 2.1\,\frac{\nu}{b}\,M_{15}^{0.36}\,h_{50}^{0.36}\ \mathrm{keV}\,, \tag{2}$$

where h_{50} is the Hubble constant in units of 50 km s^{-1} Mpc^{-1}, b is the bias parameter, ν is the number of sigma in a Gaussian distribution corresponding to the perturbation of mass M_{15} (in units of 10^{15} solar masses), and kT is the cluster gas temperature (David & Blumenthal 1991). The bias parameter, b, describes the relative distribution of visible and dark matter; b equal to one corresponds to no biasing, i.e., the dark matter fluctuation spectrum is normalized the same as that of the galaxies (at $16h_{50}^{-1}$ Mpc) and values of b greater than unity imply that the visible mass is more concentrated than the dark matter (see Dekel & Rees 1987 for a review of biasing in CDM models). As equation (2) shows, given an observed kT and a reasonable value of b, one can compute the magnitude (probability) of the perturbation from which the cluster arose in terms of its sigma in a Gaussian distribution. For $kT = 14$ keV, $M_{15} = 2.7$ and no biasing, $b = 1$, we have $\nu = 4.6$ and for $b = 1.5$, we have $\nu = 6.9$. A2163 was selected for observation with *Ginga* from the list of clusters detected by *HEAO A1* (Johnson et al. 1983). Hence, the volume from which it was drawn is conservatively less than that within $z = 0.4$. Thus, we can compute the number of clusters like A2163 we would expect to find within this volume (assuming $\Omega = 1$). For $b = 1$ and $b = 1.5$, we expect 1.5 and 10^{-6} clusters. While the statistics of finding one cluster such as A2163 are uncertain, the existence of such hot, and therefore, rare, clusters suggests that it is unlikely that b is significantly greater than 1. Earlier comparisons of biased CDM models with observations favored values of b in the range of 2–3 (Dekel & Rees 1987). However, more recent estimates favor lower values of b in the range of

1.2–1.6 (Rowan-Robinson et al. 1990 and Kaiser & Lahav 1989; see also Peebles, Daly, & Juskiewicz 1989 for a discussion of constraints on the biasing parameter b and the difficulty of reconciling a low value with observations in the context of CDM models). Deeper X-ray surveys and larger samples of clusters with measured X-ray temperatures should provide further powerful tests of CDM models (e.g., Henry & Arnaud 1991).

Note added in manuscript.—From recent observations made with the CFH Telescope (M. Arnaud, G. Soucail, & G. Mathez), the observed redshift of A2163 is 0.203, which implies a gas temperature of 13.9 keV and an X-ray luminosity of 6.4×10^{45} ergs s^{-1} in the 2–10 keV band.

We are very grateful to L. David for giving us the MPC spectrum and allowing us to quote his theoretical results before publication and to T. Dame for performing the measurements of the molecular hydrogen column density. We thank G. Blumenthal, P. Gorenstein, D. Harris, J. McClintock, D. Schwartz, and H. Tananbaum for their very useful comments on the manuscript. This work was supported by CNES and INSU and by NASA grants NAG 8-699, NAG 5-1204.

REFERENCES

Arnaud, K. A., Johnstone, R. M., Fabian, A. C., Crawford, C. S., Nulsen, P. E. J., Shafer, R. A., & Mushotzky, R. F. 1987, MNRAS, 227, 241
Arnaud, M., Lachieze-Rey, M., Rothenflug, R., Yamashita, K., & Hatsukade, I. 1991, A&A, 243, 56
Cavaliere, A., Santangelo, P., Tarquini, G., & Vittorio, N. 1986, ApJ, 305, 651
Dame, T. M., Ungerechts, H., Cohen, R. S., De Geus, E. J., Grenier, I. A., May, J., Murphy, D. C., Nyman, L. A., & Thaddeus, P. 1987, ApJ, 322, 706
David, L., & Blumenthal, G. 1991, ApJ, submitted
Dekel, A., & Rees, M. 1987, Nature, 326, 455
Edge, A. C. 1989, Ph.D. thesis, University of Leicester
Evrard, A. E. 1989, ApJ, 341, 26
Hatsukade, I. 1989, ISAS Res. Note 345
Hayashida, K., et al. 1989, PASJ, 41, 373
Henry, J. P., & Arnaud, K. A. 1991, ApJ, 372, 410
Hughes, J. P. 1989, ApJ, 337, 21
Hughes, J. P., Gorenstein, P., & Fabricant, D. 1988, ApJ, 329, 82
Hughes, J. P., & Tanaka, Y. 1991, ApJ, submitted
Johnson, M. W., Cruddace, R. G., Ulmer, M. P., Kowalski, M. P., & Woods, K. S. 1983, ApJ, 266, 425
Johnson, M. D., Bradt, H. V., Doxey, R. E., Margon, B., Marshall, F. E., & Schwartz, D. A. 1981, ApJ, 245, 799
Kaiser, N., & Lahav, O. 1989, MNRAS, 237, 129
Kowalski, M. P., Ulmer, M. P., & Cruddace, R. G. 1983, ApJ, 268, 540
Lilje, P. P. 1990, ApJ, 351, 1
Masai, K. 1984a, b, private communication, Ap&SS, 98, 367
McHardy, I. M., Stewart, G. C., Edge, A. C., Cooke, B., Yamashita, K., & Hatsukade, I. 1989, MNRAS, 242, 215
Mewe, R., Gronenshild, E. H. B. M., & van den Oord, H. J. 1985, A&AS, 62, 197
Mewe, R., Lemen, J. R., & van den Oord, H. J. 1986, A&AS, 65, 511
Mushotzky, R. F., Serlemitsos, P. J., Smith, B. W., Boldt, E. A., & Holt, S. S. 1978, ApJ, 225, 21
Peebles, P. J. E., Daly, R. A., & Juskiewicz, R. 1989, ApJ, 347, 563
Perrenod, S. C. 1980, ApJ, 236, 373
Raymond, J. C. 1985, private communication
Raymond, J. C., & Smith, B. W. 1977, ApJS, 35, 419
Rowan-Robinson, M., et al. 1990, MNRAS, 247, 1
Schaeffer, R., & Silk, J. 1988, ApJ, 333, 509
Stark, A. A., Heiles, C., Bally, J., & Linke, R. 1983, private communication
Struble, M. F., & Rood, H. J. 1987, ApJS, 63, 555
Turner, T. J., & Pounds, K. A. 1989, MNRAS, 240, 833
Turner, M. J. et al. 1989, PASJ, 41, 345
Ulmer, M. P., Kowalski, M. P., & Cruddace, R. G. 1986, ApJ, 303, 162
Warwick, R. S., Koyama, K., Inoue, H., Takano, S., Awaki, H., & Hoshi, R. 1989, PASJ, 41, 739
White, D. A., Fabian, A. C., Johnstone, R. M., Mushotsky, R. F., & Arnaud, K. A. 1991, MNRAS, in press